Modern AC Drive System with Induction Machine

Marian Gaiceanu*, and Cristian Nichita†
* Department of Automation and Electrical Engineering, Dunarea de Jos University of Galati, Romania
Marian.Gaiceanu@ieee.org
† Groupe de Recherche en Electrotechnique et Automatique du Havre, University of Le Havre, France,
nichitac@univ-lehavre.fr

Abstract— **The induction machine is widespread in AC drive system. The energy efficiency of the induction machine during dynamic regimes is up to 40%. Therefore, for the electrical drives with frequent dynamics (starting, breaking or reversing) the energy efficiency becomes a serious problem. The regenerative drive system is a solution to improve the energy efficiency in an elegant manner. This method requires of using an active front end rectifier instead of the uncontrolled rectifier, as in the conventional AC drives system. The authors proposed in this paper, a modern way to increase the energy efficiency of the drive system through the regeneration process. The power supply converter of the three-phase induction machine is designed in a modular manner, consisting of a series active power rectifier (APR), DC link, and three-phase power inverter. As regarding the DC link, the braking resistor is not necessary, the recovered energy during the braking process being delivered to the grid. Moreover, due to the used power control, DC link voltage control and current control in the grid side power converter, both the power quality and DC link capacitor minimization are ensured. The load side contains three phase voltage source inverter (VSI) in order to supply the three phase induction motor connected to the load. Through the Matlab/Simulink environment software, the obtained performances of the modular AC drive system and motoring and regenerating operation modes are shown.**

I. INTRODUCTION

Nowadays, for loads up to 250kW, the power converters with forced commutation are the best choice for a modern power converter topology supplied from 0.4 kV network. From one point of view, the AC-AC power converters are indirect AC-AC, and quasi-direct power converters, respectively. The DC-link capacitor of the indirect AC--AC power converters has the large value because the voltage source converter (VSC) and voltage source inverter (VSI) are driven independently. The most important disadvantage of the indirect current control or phase and amplitude control [1]-[2] is that of resulting of a DC offset in AC line current transients. Another control method is the predicted current control with fixed switching frequency (PCCFF) [3]-[4]. The PCCFF maintains the high dynamic performances of the hysteresis control, but is sensitive to parameter variations. Malesani et al [5]-[6] add many improvements to the hysteresis control methods. By introducing power balance control between VSC and VSI the DC link capacitor value decreases significantly [7]. The other characteristics of the quasi direct AC-AC converters (nearly input sinusoidal current, low harmonics, reduction of the energy storage devices of the system, the reactive power compensation capabilities, the kinetic energy recovery due to the reversible power flowing in AC drive applications) have been done to researchers to find and to apply large control methods.

For Voltage Source Converters (VSC) one solution to assure a fast control response to load variation is inserting of the load feedforward control [8]. The APR acts as grid interface and is used in elevators, crane, centrifuge, wind turbine drive systems.

The paper is structured in seven Sections: the first Section includes the power circuit of the modular AC drive system, the second Section describes the mathematical model of the Voltage Source Power Converter, the third Section shows the unity power factor control of the APR, the fourth Section presents the control of the Voltage Source Inverter, the fifth Section presents the Matlab/Simulink simulation results, and the conclusions could be find in the last Section.

II. THE POWER CIRCUIT OF THE MODULAR AC DRIVE SYSTEM

In the Fig. 1 the modular power converter is shown. Vector control in synchronous reference frame has been involved for the APR. Detailed methodology of control design is described. By using an adequate control design both unity power factor and increased speed loop response are obtained.

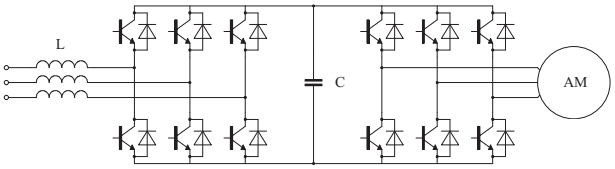

Fig. 1. Power circuit of the modular AC-AC power converter

The power structure of the regenerative drive system consists of a boost inductor, a VSC, DC-link capacitor, three-phase power inverter, a three phase squirrel cage connected to a load. In order to obtain a THD factor up to 5% at the full load the boost inductor is designed adequately. The applied methodology for the DC link capacitor design, based on maintaining the admissible DC voltage ripple, is proven through the obtained simulation results. By introducing the adequate power control loop the power balance between the load and source is maintained. The main advantage of the power balance control is the decreasing of the DC capacitor size.

III. THE MATHEMATICAL MODEL OF THE VOLTAGE SOURCE POWER CONVERTER

In the Fig. 2 the simplified diagram of the regenerative power converter is introduced.

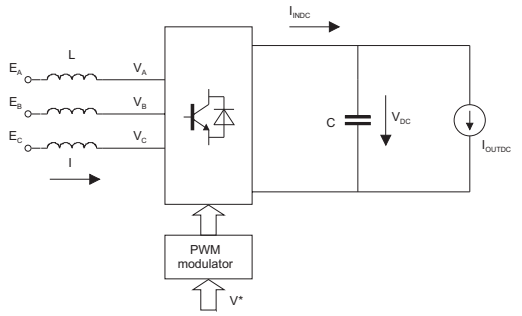

Fig. 2. Outline of the power components of the stand-alone AC power source converter with a DC load.

At the DC link output the rotor field oriented control of power inverter is connected having the current minor loop. Therefore, it can be considered as a source current connected to the DC link (Fig.2).

By applying the second Kirchhoff theorem to the input circuit (Fig.2) the stationary reference frame of the grid vector can be deducted:

$$\vec{E}_s = L\frac{d\vec{i}}{dt} + \vec{V} \tag{1}$$

where V is the converter terminal voltage, E- the source voltage, and I- the line current.
The components of the stationary grid vector are:

$$\vec{E}_s = E_\alpha + jE_\beta . \tag{2}$$

In the stationary reference frame, the components of the symmetrical grid voltage vector could be obtained as follows:

$$\begin{bmatrix} E_\alpha \\ E_\beta \end{bmatrix} = \begin{bmatrix} 1 & 0 \\ -\frac{1}{\sqrt{3}} & -\frac{2}{\sqrt{3}} \end{bmatrix} \begin{bmatrix} E_A \\ E_B \end{bmatrix} \tag{3}$$

From the eq.4 the d, q components of the synchronous reference frame are obtained:

$$\begin{bmatrix} E_D \\ E_Q \end{bmatrix} = \begin{bmatrix} \cos\omega t & -\sin\omega t \\ \sin\omega t & \cos\omega t \end{bmatrix} \begin{bmatrix} E_\alpha \\ E_\beta \end{bmatrix}, \tag{4}$$

where the instantaneous position of the grid voltage vector in the stationary reference frame is denoted by $\varepsilon = \omega t$, and $\omega = 2\pi f$ is the frequency of the grid voltage.

By multiplying the vectors in the eq. 1 with the $e^{j(\omega t - \pi/2)}$ rotate vector, the synchronous grid vector is obtained:

$$\vec{E} = \overrightarrow{E_s} e^{j(\omega t - \pi/2)} \tag{5}$$

or by using the synchronous reference frame components:

$$\vec{E} = E_Q + j \cdot E_D . \tag{6}$$

Moreover, by introducing the rotating vector term $e^{j(\omega t - \pi/2)}$ into the eq. 1, the following equation can be obtained:

$$\vec{E} e^{j(\omega t - \pi/2)} = L\frac{d\left(\vec{i}\, e^{j(\omega t - \pi/2)}\right)}{dt} + \vec{V} e^{j(\omega t - \pi/2)} . \tag{7}$$

Taking onto account the results of the eq. 6, the vectorial eq. 1 into synchronous reference frame becomes:

$$\vec{E} = L\frac{d\vec{i}}{dt} + j\omega L\vec{i} + \vec{V} . \tag{8}$$

By inserting the d, q vector components into the eq. 8, the the standard state space form of the mathematical model of the APR, in d-q synchronous reference, is obtained:

$$\begin{aligned} L\frac{dI_D}{dt} &= -\omega L \cdot I_Q - \cdot V_D + \cdot E_D \\ L\frac{dI_Q}{dt} &= \omega L \cdot I_D - \cdot V_Q + \cdot E_Q \end{aligned} \tag{9}$$

In order to deduct the entire mathematical model of the APR the additional DC link voltage equation is necessary:

$$C \cdot \frac{dV_{dc}}{dt} = I_{\mathrm{INDC}} - I_{\mathrm{OUTDC}} \tag{10}$$

It could be noted that the mathematical model contains cross-coupling terms between d, q axes (eqs.9).

The output signals of the current controllers are V_D^*, V_Q^*, which serves as the input to the pulse width modulator (PWM). Due to the switching frequency, f_{sw}, of the power semiconductors, the PWM is modeled by using the first order approximation of the Taylor series of the delay term e^{-sT_D}. Taking into account that the outputs signals of the PWM are V_D, V_Q^* the following transfer function of the PWM is considerate:

$$\begin{bmatrix} V_D \\ V_Q \end{bmatrix} = \frac{1}{1 + sT_D} \begin{bmatrix} V_D^* \\ V_Q^* \end{bmatrix} \tag{11}$$

The time constant T_D is defined as:

$$T_D = \frac{T_{sw}}{2}, \tag{12}$$

where T_{sw} is the switching time:

$$T_{sw} = \frac{1}{f_{sw}} . \tag{13}$$

The maximum voltage of the pulse width modulator depends both on the applied PWM strategy and of the available DC link voltage.

$$\left|\overline{V}\right| \le \frac{V_{DC}^{\min}}{a}, \tag{14}$$

where

$$\left|\overline{V}\right| = \sqrt{V_Q^2 + j \cdot V_D^2} \tag{15}$$

and

$$a = 1 \tag{16}$$

for space vector pulse width modulation (SVPWM) strategy, and:

$$a = \frac{2}{\sqrt{3}} \tag{17}$$

for sinusoidal pulse width modulation (SPWM).

In the Fig.3 by considering eqs. (9)-(11), the synchronous reference frame mathematical model is shown:

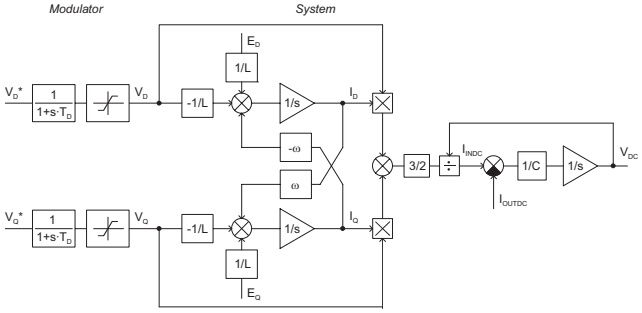

Fig. 3. The synchronous reference frame mathematical model of the APR

IV. UNITY POWER FACTOR CONTROL

The strategy of using vector control allows to the *q*, *d* synchronous reference system to be aligned with the grid voltage vector $\vec{E}$. This strategy can be obtained by using an adequate synchronization control [9]. Therefore:

$$E_D = 0\,. \tag{18}$$

In order to control independently the *d*, *q* axes the decoupled terms should be inserted into the eqs (9). In this way the independently current control is obtained.

Through the adequate current control the angle between the grid voltage vector and the input current vector becomes zero, i.e. the unity displacement factor operation is obtained.

The independently current control allows obtaining

$$I_D = 0 \tag{19}$$

if the current reference on the *d* axis is set to zero:

$$I_D^* = 0 \tag{20}$$

The unity power factor and power balance control conduct to obtaining of the load feedforward component as in [7], [9]:

$$I_Q^* = \frac{2}{3V_Q} P_{out}\,, \tag{21}$$

where P_{out} is the load power.

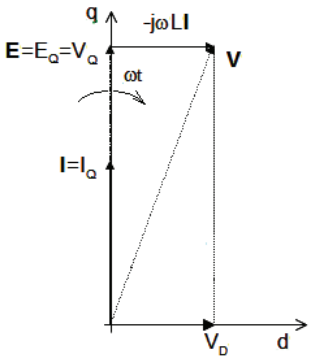

Fig. 4. Synchronous reference frame. Unity power factor.

The vector control in a cascaded manner is adopted for the APR The minor control loops consist of the *d*, *q* current regulations. The major loop of the *q* current is the DC link voltage loop.

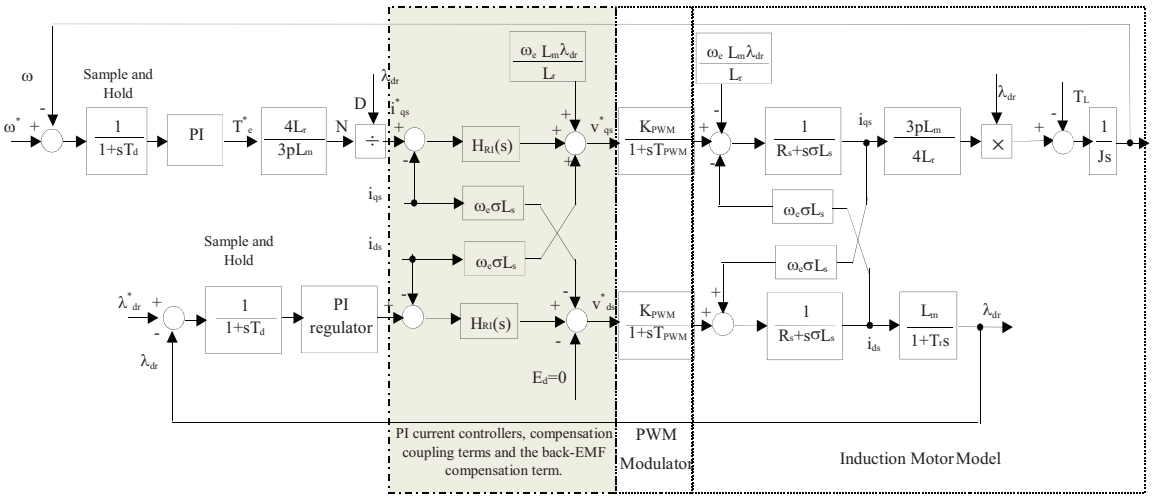

Fig.5 The rotor field vector oriented control of the AC induction machine [10].

The tuning control parameters of the Proportional Integral current controllers are determined based on the modulus optimum MO criterion as in [10]:

$$\tau_1 = T_L \tag{22}$$

$$\tau_2 = 2T_{\Sigma I} K_{PWM} K_L, \tag{23}$$

K_{PWM} is the adequate PWM gain, $T_{\Sigma I}$ - the small time constant of the current loop, $T_L=L/R$ being the time constant of the boost inductor, and $K_L=1/R$ the gain of the *R-L* load.

The parameters of the DC link PI voltage controller are determined by using the small perturbation linearization method of the link voltage equation around the equilibrium point [11].

V. INDUCTION MACHINE CONTROL

In order to follow the speed reference the vector control in rotor magnetizing synchronous reference frame has been used. The cascaded control loops are used [12]. The *q* axis control consists of the torque (current) control and speed control. The *d* axis control consists of the rotor magnetizing current control, that is the flux control [10]. The rotor field vector control is used to decouple the magnetic side from the mechanical side of the three-phase induction machine.

The mathematical model of the three-phase induction machine in synchronous reference frame consists of the *d*, *q* stator voltage differential equations, rotor magnetizing differential equation, the equation of the oriented control mechanism, and circular motion equation:

$$\begin{aligned}
&\sigma T_s \frac{di_{ds}}{dt} + i_{ds} = \frac{v_{ds}}{R_s} - (1-\sigma) T_s \frac{di_{mR}}{dt} + \sigma T_s \omega_e i_{qs} \\
&\sigma T_s \frac{di_{qs}}{dt} + i_{qs} = \frac{v_{qs}}{R_s} - (1-\sigma) T_s \omega_e i_{mR} - \sigma T_s \omega_e i_{ds} \\
&\frac{di_{mR}}{dt} = \frac{1}{T_r}\left(-i_{mR} + L_m i_{ds}\right) \\
&J \frac{d\omega_r}{dt} = k_T i_{mR} i_{qs} - T_L, \quad K_T = \frac{2}{3}(1-\sigma) L_s \\
&\omega_e = \omega_r + \omega_{sl}, \quad \omega_{sl} = \frac{R_r}{L_m} \frac{i_{qs}}{i_{mR}}
\end{aligned} \tag{24}$$

where:

R_s - stator resistance per phase

ω_e synchronous rotating frame angular speed.

ω_r rotor angular speed.

ω_{sl} slip angular speed.

i_{ds} (i_{qs}) *d*-axis (*q*-axis) stator current.

v^*_{ds} (v^*_{qs}) *d*-axis (*q*-axis) stator voltage commands.

L_s (L_r) - the stator (rotor) inductance

L_m - the mutual inductance.

$T_s=L_s/R_s$ the time constant of the stator circuit.

σ the total leakage factor.

T_L the total load torque.

$T_r=L_r/R_r$ the time constant of the rotor circuit.

K_T torque constant

J the moment of inertia.

p-the number of poles pairs.

In order to assure an independent control of the three-phase induction machine the adequate decoupling voltage components are inserted [13].

The parameters of the PI torque regulator deducted by using modulus optimum are as follows [14], [15]:

$$\begin{aligned}
\tau_{1c} &= \frac{\sigma L_s}{R_s} \\
\tau_{2c} &= 2T_{eI} K_{PWM} \frac{1}{R_s}
\end{aligned} \tag{25}$$

where the time constant $T_{eI}=1{,}5T_s$ is multiple of the sampling period T_s [11].

By using symmetrical optimum criterion [12] the parameters of the PI speed regulator are found:

$$\begin{aligned}
\tau_3 &= 4T_{\Sigma s} \\
\tau_4 &= \frac{8T_{\Sigma s}^2}{J}
\end{aligned} \tag{26}$$

where the smallest time constants are grouped into $T_{\Sigma s}=2T_{eI}+T_d$ time constant.

VI. SIMULATION RESULTS

The proposed regenerative power system taken into consideration has the following data: S_n=22kVA -rated apparent power, I_n=31.75A- rated current, the parametrers of the input inductance R_{in}=0.001Ω, L_{in}=2.1mH, and the DC-link capacitor C=1565uF. The load of power system is connected to the three-phase induction machine (IM). The load power (Fig.8) consists of an elevator connected to the IM: P_n= 4 [kW], n_N=1900 [rpm] rated speed, T_l= 19 [Nm] rated load torque. In the Fig. 6 the Matlab/Simulink software implementation of the entire AC drive system is shown. In the Figs 7-15 the numerical simulation results are shown. For an elevator, the considerate speed cycle consists of the starting, steady state speed, braking, and a rest time (Fig.7).

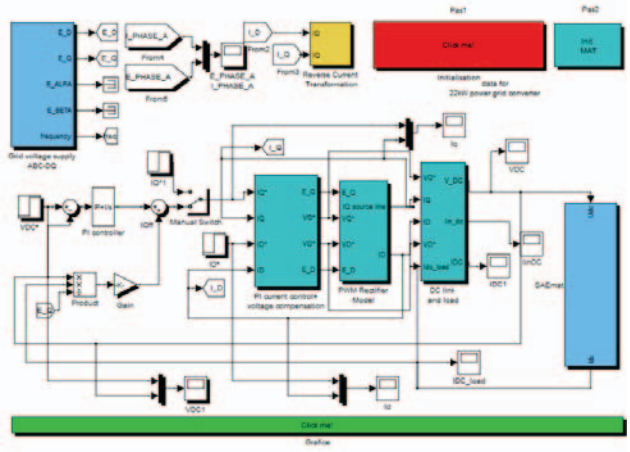

Fig. 6. Simulink implementation of the AC regenerative drive system

The designed controller parameters conduct to the perfect reference tracking of the feedback speed, therefore the reference speed and the current speed are overlapped entirely (Fig.7). The active load torque is applied at 0.25 [s]

(Fig.8). During the transients the electromagnetic torque of the three-phase induction machine attains the maximum value.

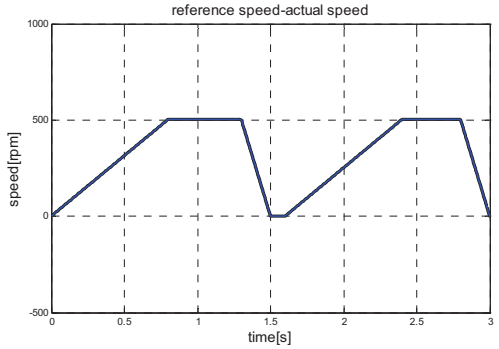

Fig.7. Speed regulator: reference speed and the actual speed

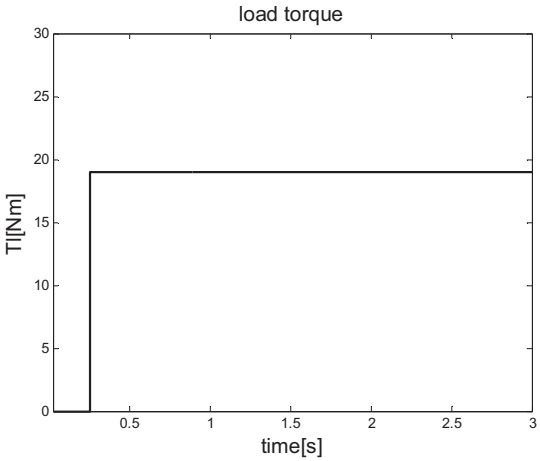

Fig.8. The torque diagram of the elevator

In the Fig. 8 the active load torque is shown. During the dynamic regimes, by using the appropriate control the maximum load torque is obtained (Fig.9). During the steady state the electromagnetic torque and the load torque have the same values (Fig.9). The regeneration regimes appear during braking process, the electromagnetic torque changing the sign (Fig.9).

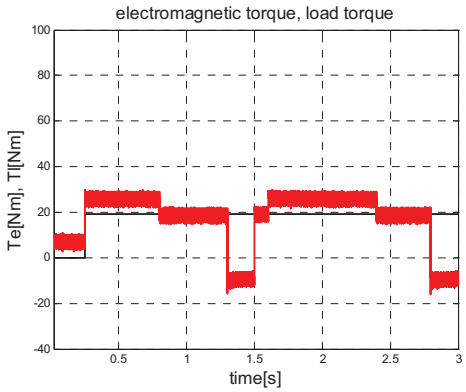

Fig.9. The electromagnetic torque of the IM machine

The modular AC electrical drive system operates in the regeneration mode during braking process (t∈[1.3, 1.5]s and [2.8, 3]s) : the negative active current reference is generated (Figs.10), the grid current and grid voltage are out of phase by 180^o (Fig.12), and the DC overvoltage occurs during braking time (Fig.13). In the Figs.14, 15 the magnified pictures during braking period are shown. During the braking period the IM acts as generator and delivers the electrical energy from the elevator to the grid, that is the mechanical energy from the elevator is recovered, and it is delivered through the IM into the AC line.

The active current controller performances are shown in the Fig. 10. The feedback active current follows accurately the reference one. In the Fig.11 the performances of the *d* axis current controller are shown. In order to obtain a unity power factor, the *d* axis current is set to zero (Fig.11).

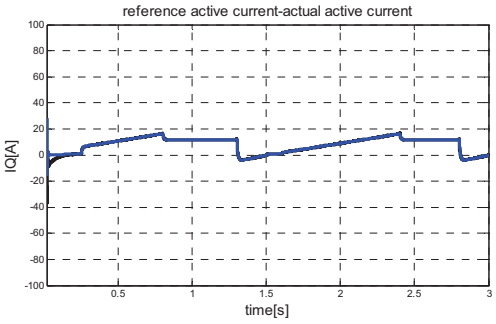

Fig.10. *d* axis current controller: the reference and the feedback active current

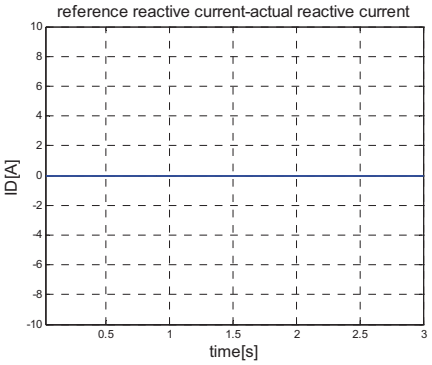

Fig. 11. *q* axis current controller: the reference and the feedback reactive current

The phase (*A*) of the grid current is in phase with the corresponding phase of the grid voltage (*A*), and out of phase in regeneration mode. Therefore, the unity power factor operation in motoring mode and regeneration mode are shown (Figs. 12, 14).

In order to assure a reversibility of the load current the DC bus voltage V_{DC} becomes higher than of the reference DC voltage (Fig.13).

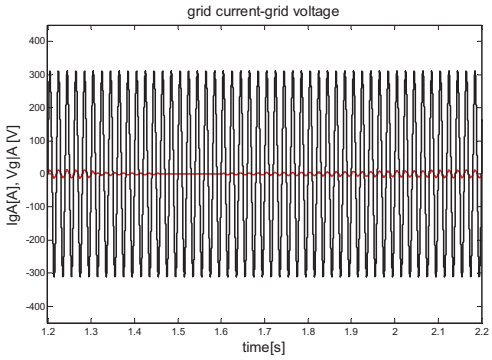

Fig.12. Unity power factor operation in motoring and regenerating mode of operations

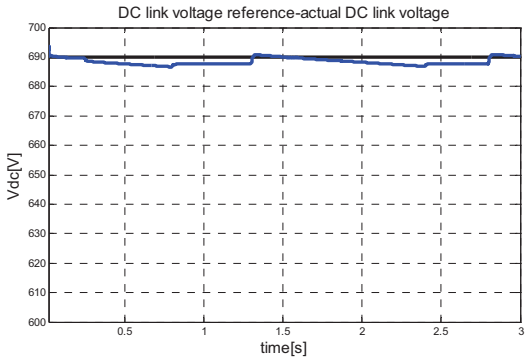

Fig.13. DC link voltage controller

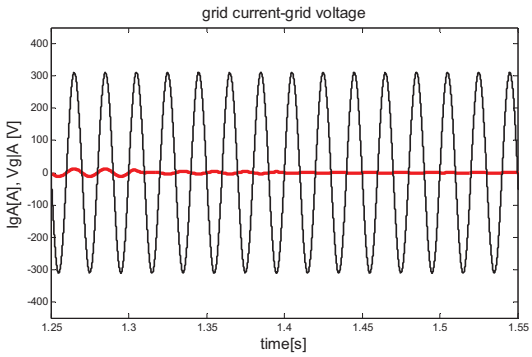

Fig.14. The unity power factor operation during the motoring and regeneration operation modes(magnified area).

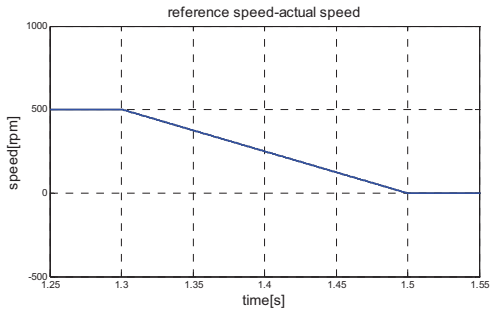

Fig.15. The speed of the IM: braking process (magnified area).

VII. CONCLUSION

The topology, mathematical modeling, control design and numerical simulation results of the modern IM drive system have been shown in this paper. The advantages of the modular topology with the described control strategies are: sinusoidal input current, unity power factor, bidirectional power flow, small (up to 5%) DC-link voltage variation in any operated conditions, disturbance compensation capability, fast control response and high quality balanced three-phase output voltages were obtained. The power balance control delivers the load feed-forward component which is added to the input reference of the active current. In this way a better transient response is obtained. The response time speed of the active current loop allows the reduction of the size of the DC link capacitor at the same time with maintaining the systems' stability.

The simulation results on the 22-kVA, 400V regenerative power unit confirm the good load current regulation, the unity power factor operation of the power source converter, power reversibility capabilities as well as the good power matching control. During the braking process the mechanical energy is fed to the grid. In this way, the increased efficiency of the AC drive system is obtained. Moreover, during the braking process the AC line current decreases. Therefore, the dissipated energy into the active elements of the AC drive system is diminished. In this way the entire efficiency of the drive system increases more.

ACKNOWLEDGMENT

This work was supported by a grant of the Romanian National Authority for Scientific Research, CNDI–UEFISCDI, project number PN-II-PT-PCCA-2011-3.2-1680.

REFERENCES

[1] J. W. Dixon and B.T.Ooi: " Indirect Current Control of a Unity Power Factor Sinusoidal Current Boost Type Three-Phase Rectifier", IEEE Trans on Ind. Electronics, vol. 35, No. 4, pp. 508-515, Nov/Dec. 1988

[2] R.Wu, S.B.Dewan, and G.R. Slemon, "Analysis of an ac to dc voltage source converter using PWM with phase and amplitude control", in Conf. Rec. IEEE-IAS, 1989

[3] R. Wu, S.B. Dewan, and G.R.Slemon, "Analysis of a PWM AC to DC voltage source converter under the predicted current", IEEE Trans on Ind. Appl., vol.27, no.4, pp.756-764, July/Aug. 1991

[4] Sonaglioni, L.: "Predictive digital hysteresis current control," Industry Applications Conference, 1995. Thirtieth IAS Annual Meeting, IAS '95., Conference Record of the 1995 IEEE , vol. 3 , pp. 1879 -1886 8-12 Oct. 1995

[5] Malesani, L., Tenti, P. "A novel hysteresis control method for current controlled VSI PWM inverters with constant modulation frequency", vol.26, pp.88-92 , Jan./Feb. 1990

[6] Malesani, L., Mattavelli, P., and Tomasin, P. "Improved constant frequency hysteresis current control of VSI inverters with simple feed-forward bandwidth prediction ", Orlando, FL, pp.2633-2640, Oct. 1995

[7] R. Uhrin, F. Profumo, "Stand alone AC/DC converter for multiple inverter applications," Power Electronics Specialists Conference, 1996. PESC '96 Record, 27th Annual IEEE, Vol. 1, 23-27 June 1996, pp. 120 -126

[8] M. Gaiceanu, Inverter Control for Three-Phase Grid Connected Fuel Cell Power System, Compatibility in Power Electronics, 2007. CPE '07, Digital Object Identifier: 10.1109/CPE.2007.4296506, Publication Year: 2007, Page(s): 1 - 6

[9] M. Gaiceanu, Quasi-Direct PWM AC-AC Converter Solution for AC Drives pg.225 , "Przegląd Elektrotechniczny" (Electrical Review, 2010

[10] M. Gaiceanu, Regenerative AC drive system with Three-phase Induction Machine, 2014 International Conference on Applied and Theoretical Electricity (ICATE), ISBN 978-1-4799-4161-2/14, 2014, 23-25 Oct, Craiova, Romania

[11] M. Gaiceanu, G. Fetecau, Grid connected Wind turbine-Fuel Cell Power System having Power Quality Issues, EPQU'07 Barcelona, pp.7-13, 2007. ISBN 978-84-690-9441-9

[12] Leonhard, W., Control of electrical drives, Springer-Verlag, Berlin, 1996

[13] M. Kazmierkowski, Control in Power Electronics: Selected Problems, 2002, Academic Press – Elsevier

[14] I. Dumitrache, S. Dumitriu, I.Mihnea, F. Munteanu, Gh. Musca, and C. Calcev, "Automatizari electronice" (Electronics automation), Didactic and Pedagogical Publishing House, Bucuresti, 1993

[15] C. Bajracharya, M. Molinas, J. A. Suul, and T. M. Undeland, Understanding of tuning techniques of converter controllers for VSC-HVDC NORPIE/2008, Nordic Workshop on Power and Industrial Electronics, June 9-11, 2008, CD pp1-8